TECHNICAL UNIVERSITY OF CLUJ-NAPOCA

ACTA TECHNICA NAPOCENSIS

Series: Applied Mathematics, Mechanics, and Engineering
Vol. 60, Issue I, March, 2017

EXPERIMENTAL POWER DETERMINATION OF A GAMMA TYPE STIRLING ENGINE

Adrian Ioan BOTEAN, Iacob HITICAŞ

Abstract: *In this study, aims to determine the experimental power output of a gamma-configuration Stirling engine, with a displacement of 38.16 cm^3 in operating mode corresponding to partial loads, respectively, to total loads. The braking element is the DC electric generator and partial loads are three electrical resistances respectively short-circuit operation of the electric engine. For electric engine operation in full load regime it is supplied with electricity through a variable voltage sources. Are drawn diagrams variance hot source, cold source and vary the speed and power in total and partial loads.*

Key words: *Stirling engine, type Gamma, temperature hot source, cold source temperature, speed, power, DC engine*

1. INTRODUCTION

In the middle of a crisis for finding alternative energy sources, the Stirling engine is a real solution. It has drawn the researchers' attention due to the advantages it offers. Low gas emission and higher efficiency in comparison with internal combustion engines are just the first advantages to be mentioned from a generous list.

The Stirling engine is an external combustion engine with regenerative, closed-cycle. It operates by cycles of compression and decompression of a working fluid. It's based on temperature differences and it converts thermal energy into mechanical energy.

Stirling engine's key element relates to the use of a heat exchanger [3, 8] which causes a high yield potential.

The motor cycle is closed and thus it contains a specified quantity of gas (a constant quantity) which is called the working fluid. Air, hydrogen and helium are the most commonly used as working fluids.

Unselective in terms of the source of heat, the Stirling engine uses any fuel or heat source, including solar energy [16].

The Stirling engine was patented in 1816 by Robert Stirling. Over the years, a number of models and variants, numerical and / or experimental were made [4, 5, 6, 7]. In addition, optimization methods and algorithms have also been created [13, 14, 15].

Karabulut [6] has addressed the problem of determining the experimental power of a Stirling engine. He has even demonstrated that the relationship between the final temperature of the hot heat source and the engine's power seems to be linear.

Chen [7] made a series of experiments and measurements on a Gamma type Stirling engine and concluded that the engine's output power depends on its speed (number of revolutions in rot/min).

Sripakagorn [10] proposes finding the Stirling engine's power based on its torque and speed, with the engine being connected to a DC electric generator. The latter is charged by an variable electrical resistance. In order to measure the shaft power, the generator is attached to an arm torsion which allows the measurement of the torque through a calibrated scale.

Several numerical methods and mathematical models were developed in order to design a Stirling engine and to determine different operating parameters. These analytical methods and models: the method of Schmidt, the

number of Beale, West's formula, the formula of medium pressure, Malmo formula [5].

Numerical methods show relatively large errors during the practical realization. Experimental studies have helped providing useful data for analytical and numerical models' calibration.

In general, the experimental power determination is realized by knowing the developed engine torque and its speed.

The present study aims to determine the experimental power output of a Gamma type Stirling engine, with a volume of 38.16 cm3, by pairing it to a DC electric generator and comparing this power with the results obtained analytically in the study [19].

2. METHODS

Experimental stand from Figure 1 consists of a Gamma type Stirling engine. Compared to the initial configuration [19] three more cooling coils were added. These coils are made of copper tubes with water circulating inside, at a certain rate, controlled through a valve. This assembly represents the Stirling engine's cooling system.

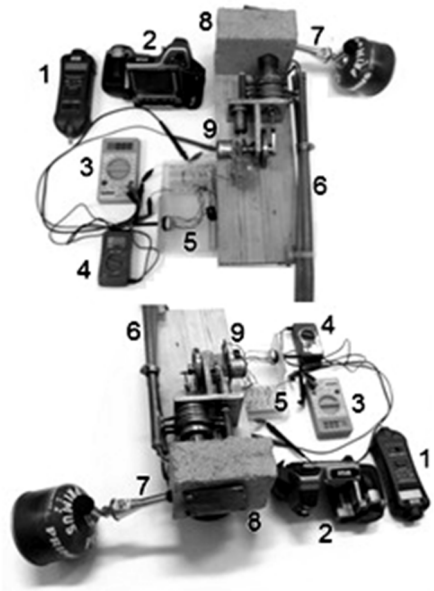

Fig.1 Experimental stand consists of: 1 - tachometer; 2 – thermal camera; 3 - ammeter; 4 - voltmeter; 5 - breadbord and electric resistors; 6 – cooling system; 7 - burner; 8 - refractory bricks; 9 – DC electric generator.

The supply of thermal energy is provided by a burner using a canister of gas. The burner is introduced inside an enclosure made of refractory bricks, aiming to minimize heat loss. On the flywheel, a DC electric generator shaft is attached. This one is charged using an electrical resistance (22, 56 and 100 ohms) connected to a breadboard and interchanged with a rotary switch, according to Figure 2.

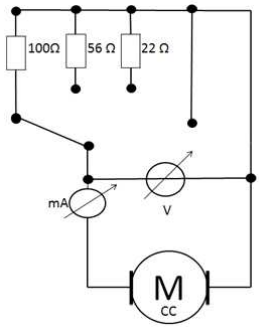

Fig.2 The wiring diagram showing the load of the DC electric generator.

The output power of the Stirling engine can be determined by using the relation

$$P=U\cdot I \ [W]$$

which is why, in the circuit of Figure 2, a voltmeter was introduced to determine the potential difference (voltage). In addition, an ammeter is used to determine the electric current.

The thermal camera (Flir T400) monitors the temperature (in degrees Celsius) of both the hot and the cold source. The tachometer (DT-1236L) measures the flywheel rotation (in rot/min).

3. RESULTS

Figure 3 shows the diagram of the variation of temperature of the hot source. It is time related and provides three sets of measurements. From this diagram we can see that after a lapse of about 30 minutes, the Stirling engine records a state of thermal equilibrium, with its speed becoming constant.

Figure 4 presents the variation registered in the speed of the flywheels (expressed in rot/mim), first when spinning in void, and then charged with he help of three electrical resistances (according to Fig.2). The same chart highlights the change of the speed when the operating mode is the short circuit of the DC electric generator.

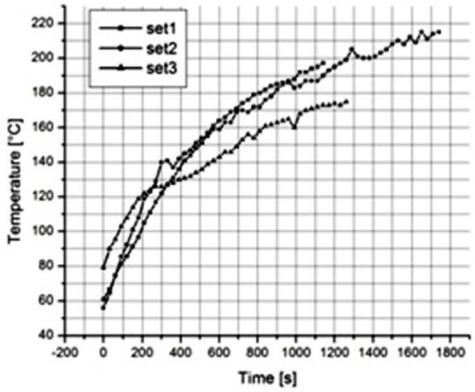

Fig.3 Diagram of hot source temperature variation, time - related.

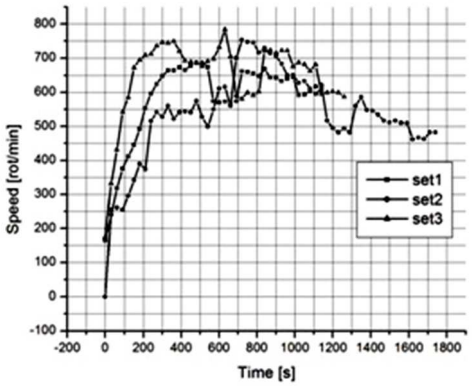

Fig.4 The diagram of speed variation versus time.

In Figure 5 are shown, in detail, the changes of the speed related to set no.3 of measurements. Each set of measurements starts with the hot source temperature taken from ambient temperature, it continues with heating and it and ends with its complete cooling.

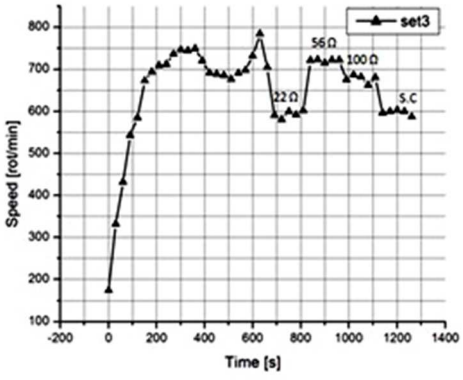

Fig.5 The diagram of the variation of speed versus time, for set no.3 of measurements.

Using the calculation formula for the electrical power has led to the diagram of variation of the Stirling engine'spower, depending on the load applied to the three sets of tests, according to Figure 6.

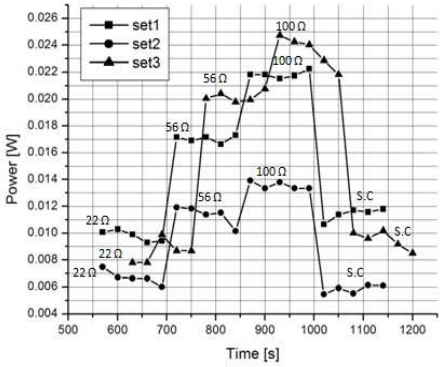

Fig.6 The variation of power – time - related.

For the same loading configuration (see Fig.2), the hot source was heated (Fig.3) until the Stirling engine reached the state of thermal equilibrium. Figure 7 shows the diagram of the cold source's variation of temperature versus time. It followed a number of three cycles of successive requests: connecting the three electrical resistances, respectively, short-circuit condition, and obtaining a modification of the Stirling engine speed, according to Figure 8.

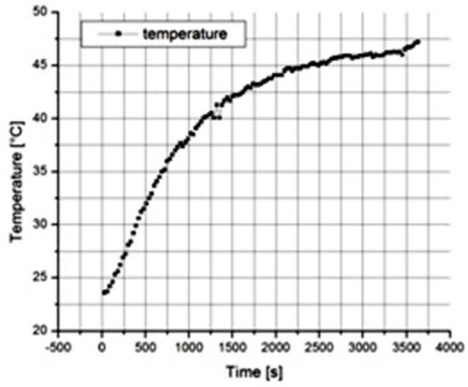

Fig.7 The diagram of cold source temperature variation with time.

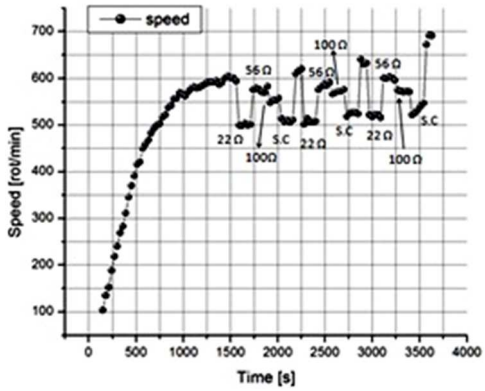

Fig.8 The diagram of speed variation versus time, for three load cycles.

Figure 9 depicts the diagram of the power variation – time - related – for the three load cycles considered.

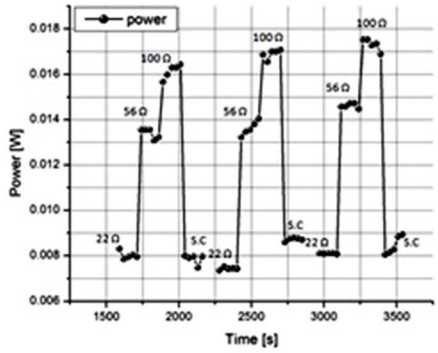

Fig.9 The diagram of power variation – time - related – for the three load cycles.

It was found that putting the DC electric generator in load by using electrical resistances of 22Ω, 56Ω, 100Ω and, as well as functioning in short circuit, does not lead to a full braking of the Stirling engine. Consequently, it failed to determine the maximum power developed.

To obtain the full brakingof the Stirling engine, the electrical motor was connected to a DC power source, with variable voltage. The wiring diagram is shown in Figure 10.

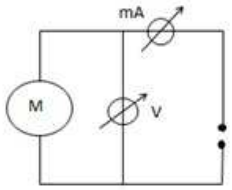

Fig.10 Wiring diagram to connect the DC electric engine to a variable voltage source.

By varying the supply voltage of the electric engine, the latter will produce a Stirling engine braking effect until completely braked (speed reaches zero value).Then, we record the voltmeter and ammeter readings, and their product is the power developed by the Stirling engine, according to Figure 11.

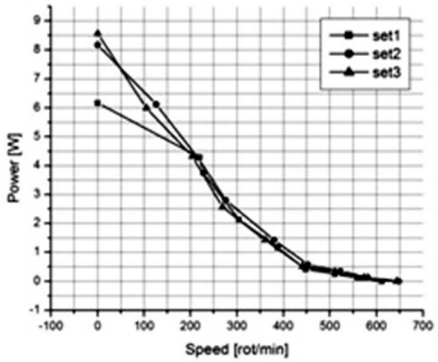

Fig.11 The diagram of Stirling engine power variation depending on speed.

4. CONCLUSIONS

The Stirling engine reaches a thermal equilibrium (hot source temperature is between 200 and 220 degrees Celsius and cold source temperature of about 45-50 degrees Celsius, according to Figure 3 and Figure 7) after about 30 minutes, and wheel speed flywheels average approximately 650 rotations per minute, according to data presented in Figure 4. By coupling the electrical circuit in Figure 2 the resistors and operation of the electric motor in short-circuit conditions can be seen from Figure 4 that there is a period of time of about 60 seconds is needed to change from one speed range to another. For a more detailed analysis of the change in speed increments depending on the task, in Figure 4 is considered, for example, set no.3 of measurements highlighted in Figure 5. Of this figure shows that when Stirling engine reaches a state of thermal equilibrium, speed is about 750 rpm. If the circuit in Figure 2 is coupled in electrical resistance of 22 ohms will reach the speed of 600 rotation per minute; for the resistance of 56 ohmi, speed reaches about 750 rotations per minute; for the resistance of 100 ohms reaches the speed of about 680 rotations per minute and when the motor is operated continuously short-circuit reaches the speed of about 600 rotations per minute. It is noted that the DC electric generator in loads has not completely breaks Stirling engine, this operating mode can be considered a system of intermediate tasks. In this case the power developed by the engine Stirling is 0.01 to 0.025 watts for the three sets of measurements, according to Figure 6. Also in Figure 6 is registered differences between the powers obtained for the no.3 measurements. This is caused because each set of measurements, Stirling engine has warmed until thermal equilibrium was recorded, and after commissioning task has cooled, and the three sets of measurements are not entirely identical in terms of initial heating temperature. For this reason it proceeded to achieving a set of measurements in which the task has changed (see Fig.2) after three cycles of loads. In Figure 8 is shown the diagram speed variation for the

three load cycles in funt size load (electrical resistance) applied, observing behavior identical to the three cycles, slightly upward. This means that not yet completely reached a state of thermal equilibrium. The variation in the three load cycles is represented in Figure 9. The maximum power developed is approximately 0.017 watts. Total power provided by the Stirling engine is determined fueling the DC engine from a current source and voltage variable according to wiring diagram in Figure 10. In Figure 11 is plotted diagram of variation of the total power, the maximum being about 8.5 watts. The difference of total power output diagram (Fig.11) and Schmidt's method [19] is almost 10 times. Such a difference can be explained by local pressure losses in the system due to leaks between hard elements are in motion.

5. ACKNOWLEDGEMENTS

This study was made possible by the technical support given by PhD. Eng. Fechete Lucian, lecturer at the Automotive Engineering and Transportations Department, Faculty of Mechanics, Technical University of Cluj-Napoca.

6. REFERENCES

[1] Dragomirescu G.T., Optimizarea exergoeconomică a sistemelor de trigenerare a energiei, Teza de doctorat, Bucureşti, 28 septembrie 2012, pp. 128.

[2] Petrescu F.I.T., Teoria Mecanismelor. Curs şi aplicaţii, USA, September 2012, pp. 38-40, ISBN 978-1-4792-9362-9.

[3] Gheith R, Aloui F., Nasrallah S.B., Study of the regenerator constituting material influence on a gamma type Stirling engine, Journal of Mechanical Science and Technology, 26 (4) 2012, pp. 1251-1255.

[4] Çinar.C, Karabulut H., Manufacturing and testing of a gamma type Stirling engine, Renewable Energy 30 (2005), pp. 57–66.

[5] Kongtragool B., Wongwises S., Investigation on power output of the gamma-configuration low temperature differential Stirling engines, Renewable Energy, 30 (2005), pp. 465–476.

[6] Karabulut H., Çinar C., Oztürk E., Yücesu H.S., Torque and power characteristics of a helium charged Stirling engine with a lever controlled displacer driving mechanism, Renewable Energy 35 (2010), pp. 138–143.

[7] Chen W.L., Wong K.L., Po L.W., A numerical analysis on the performance of a pressurized twin power piston gamma-type Stirling engine, Energy Conversion and Management, 62 (2012), pp. 84–92.

[8] Timoumi Y., Tlili I., Nasrallah S.B., Design and performance optimization of GPU-3 Stirling engines, Energy 33 (2008), pp. 1100–1114.

[9] Toghyani S., Kasaeian A., Ahmadi M.H., Multi-objective optimization of Stirling engine using non-ideal adiabatic method, Energy Conversion and Management, 80 (2014), pp. 54–62.

[10] Sripakagorn A., Srikam C., Design and performance of a moderate temperature difference Stirling engine, Renewable Energy, 36 (2011), pp. 1728-1733.

[11] Ahmadi M.H., Ahmadi M.A., Pourfayaz F., Bidi M., Hosseinzade H., Feidt M., Optimization of powered Stirling heat engine with finite speed thermodynamics, Energy Conversion and Management, 108 (2016), pp. 96–105.

[12] Hooshang M., Moghadam R.A., Nia S.A., Dynamic response simulation and experiment for gamma-type Stirling engine, Renewable Energy 86 (2016), pp. 192-205.

[13] Gheith R., Hachem H., Aloui F., Nasrallah S.B., Experimental and theoretical investigation of Stirling engine heater, Parametrical optimization, Energy Conversion and Management, 105 (2015), pp. 285–293.

[14] Féniès G., Formosa F., Ramousse J., Badel A., Double acting Stirling engine. Modeling, experiments and optimization, Applied Energy, 159 (2015), pp. 350–361.

[15] Luo Z., Sultan U., Ni M., Peng H., Shi B., Xiao G., Multi-objective optimization for GPU3 Stirling engine by combining multi-objective algorithms, Renewable Energy, 94 (2016), pp. 114-125.

[16] Ahmadi M.H., Ahmadi M.A., Mellit A., Pourfayaz F., Feidt M., Thermodynamic

analysis and multi objective optimization of performance of solar dish Stirling engine by the centrality of entransy and entropy generation, Electrical Power and Energy Systems 78 (2016) 88–95.

[17] Alfarawi S., AL-Dadah R., Mahmoud S., Enhanced thermodynamic modelling of a gamma-type Stirling engine, Applied Thermal Engineering, 106 (2016), pp. 1380–1390.

[18] Demir B., Gungor A., Manufacturing and testing of a v-type Stirling engine, International Journal of Electronics, Mechanical and Mechatronics Engineering, Vol.1. No.1, 2010, pp. 39-44.

[19] Botean A.I., Florescu M., Glogoveţan A., Vitan V., The functional analysis of a gamma type Stirling engine, Acta Technica Napocensis, Series: Applied Mathematics, Mechanics, and Engineering, Vol. 59, Issue I, March, 2016, pp. 53-58.

Determinarea experimentală a puterii unui motor Stirling de tip Gamma

Rezumat: *În prezentul studiu se urmăreşte determinarea experimentală a puterii unui motor Stirling de tip Gamma, având o cilindree de 38.16 cm^3, în regim de funcţionare corespunzător unor sarcini parţiale respectiv, a unor sarcini totale. Elementul de frânare îl constituie un motor de curent continuu iar sarcinile parţiale sunt în număr de trei rezistenţe electrice respectiv funcţionarea în regim de scurtcircuit a motorului electric. Pentru funcţionarea motorului electric în regim de sarcină totală acesta se alimentează cu curent electric prin intermediul unei surse variabile. Sunt trasate diagramele de variaţie a temperaturii sursei calde, a sursei reci precum şi variaţia turaţiei şi a puterii în regim de sarcini parţiale şi totale.*

Adrian Ioan BOTEAN, Lecturer, Ph.D., Technical University of Cluj-Napoca, Department of Mechanical Engineering, 103-105 Muncii Blvd., 400641, Cluj-Napoca, +40-264-401751, Adrian.Ioan.Botean@rezi.utcluj.ro.

Iacob HITICAŞ, Student, Automotive Engineering and Transportations Department, Faculty of Mechanics, Technical University of Cluj-Napoca, 103-105 Muncii Blvd, 400641, Cluj-Napoca.